Research Square

Preprints are preliminary reports that have not undergone peer review.
They should not be considered conclusive, used to inform clinical practice,
or referenced by the media as validated information.

NAP1L1 Interacts with Hepatoma-Derived Growth Factor to Recruit C-Jun Inducing Breast Cancer Growth

Shu Liu (3543359430@qq.com)
Guizhou Medical University
Yewei Zhang
Guizhou Medical University
Shien Cui
Southern Medical University Nanfang Hospital
Bo Li
Guizhou Medical University
Qian Chen
Guizhou Medical University
Guangyu Yao
Southern Medical University Nanfang Hospital
BIN GONG (gb18573204146@163.com)
Southern Medical University https://orcid.org/0000-0003-4446-4280

Primary research

Keywords: Breast cancer, oncogene, NAP1L1, HDGF, C-JUN

Posted Date: May 17th, 2021

DOI: https://doi.org/10.21203/rs.3.rs-462163/v1

License: This work is licensed under a Creative Commons Attribution 4.0 International License.
Read Full License

Version of Record: A version of this preprint was published at Cancer Cell International on November 13th, 2021. See the published version at https://doi.org/10.1186/s12935-021-02301-3.

Abstract

Background Breast cancer is the top cancer in women in the world. However, its pathogenesis is still to be determined. The role and molecular mechanism of NAP1L1 in breast cancer have not been reported. Elucidation of molecular mechanism might provide a novel therapeutic target for glioma treatment.

Methods A bioinformatics analysis was conducted to determine the differential expression of NAP1L1 in breast cancer and find the potential biomarker that interacts with NAP1L1 and HDGF. The expression of NAP1L1 in tissues was detected by using immunohistochemistry. Breast cancer cells were transfected with the corresponding lentiviral particles and siRNA. Then, MTT, Edu, plate clone formation, and subcutaneous tumorigenesis in nude mice were used to detect the cell proliferation in breast cancer. Furthermore, coimmunoprecipitation (Co-IP) assay and confocal microscopy were performed to explore the detailed molecular mechanism of NAP1L1 in breast cancer.

Results In this study, Nucleosome Assembly Protein 1 Like 1 (NAP1L1) protein was upregulated based on the Clinical Proteomic Tumor Analysis Consortium (CPTAC) database. Consistent with the prediction, immunohistochemistry staining showed that NAP1L1 protein expression was significantly increased in breast cancer tissues. Its elevated expression was an unfavorable factor for breast cancer clinical progression and poor prognosis. Stably or transiently knocking down NAP1L1 reduced the cell growth *in vivo* and *in vitro* via repressing the cell cycle signal in breast cancer. Furthermore, the molecular basis of NAP1L1-induced cell cycle signal was further studied. NAP1L1 interacted with the hepatoma-derived growth factor (HDGF), an oncogenic factor for tumors, and the latter subsequently recruited the key oncogenic transcription factor c-Jun, which finally induced the expression of cell cycle promoter CCND1 and thus the cell growth of breast cancer.

Conclusions Our data demonstrated that NAP1L1 functions as a potential oncogene via interacting with HDGF to recruit c-Jun in breast cancer.

1. Introduction

Breast cancer is a serious disease in which malignant cells are formed in breast tissues. It is the second most common cancer in women after skin cancer. The etiology of breast cancer is still unclear, which may be related to the patient's age, family history, hormone, long-term excessive drinking, and carrying mutation genes related to breast cancer. These factors alone or together induce the abnormal expression of some genes[1–6] and thus promote the pathogenesis of breast cancer.

Nucleosome Assembly Protein 1 Like 1 (NAP1L1) belongs to a member of the nucleosome assembly protein (NAP) family[7]. It is involved in DNA replication[8] and may play a role in regulating chromatin formation and contribute to the modulation of cell growth[9]. In previous studies, NAP1L1 has been shown as a potential tumor promoter and participated in the pathogenesis of several tumors including colorectal

cancer, renal cancer, liver cancer, and pancreatic neuroendocrine neoplasm[10–14]. Yet, the role and molecular mechanism of NAP1L1 in breast cancer have not been reported.

Here, NAP1L1 protein was found to be upregulated and considered as an unfavorable factor for the poor progression and prognosis of breast cancer patients. Furthermore, NAP1L1 was observed to be an interaction factor of hepatoma-derived growth factor (HDGF), recruiting the key oncogenic transcription factor c-Jun and thus inducing the expression of cell cycle promoter CCND1, which finally stimulated breast cancer proliferation. These detailed data indicate NAP1L1 as a potential oncogene, significantly participating in the pathogenesis of breast cancer.

2. Materials And Methods

2.1 Bioinformatics assay

BIOGRID web (https://thebiogrid.org/) was used to find the potential biomarker interaction with NAP1L1 and HDGF. UALCAN web (http://ualcan.path.uab.EdU/) was used to analyze the differential protein expression of NAP1L1 in breast cancer based on the analysis of Clinical Proteomic Tumor Analysis Consortium (CPTAC) database.

2.2 Cell culture

Two breast cancer cell lines (MCF-7 and MDA-MB-231) were obtained from the Cell Bank of the Chinese Academy of Science (Shanghai, China). MDA-MB-231 cell lines were cultured in Dulbecco's modified Eagle medium (DMEM) (PAN-Biotech, Aidenbach, Germany). MCF-7 cell lines were cultured in Roswell Park Memorial Institute-1640 (RPMI-1640) (PAN-Biotech, Aidenbach, Germany). All cell lines were incubated in a 5% CO_2 humidified chamber at 37℃ and supplemented with 10% fetal bovine serum (FBS; PAN-Biotech, Aidenbach, Germany) .

2.3 Immunohistochemistry

Breast cancer tissue microarray (TMA) was purchased from Shanghai Outdo Biotech (Shanghai Outdo Biotech, Shanghai, China). They were used to evaluate the NAP1L1 protein expression. Consent from the patients and approval from the Ethics Committee of Shanghai Outdo Biotech were obtained before using the clinical samples for research purposes. Tissue sections from the *in vivo* experiments were used to detect Ki67 and PCNA protein expression levels using immunohistochemistry. The antibodies used were rabbit anti-PCNA (1:200; Proteintech, Rosemont, USA) and mouse anti-Ki67 (1:200; Signalway Antibody, Maryland, USA). The indirect streptavidin-peroxidase method was used according to the manufacturer's standard experiment guidelines. Cell staining was respectively scored by two pathologists blinded to the clinical parameters. The extent of staining, defined as the percentage of positively stained tumor cells in relation to the whole tissue area, was scored on a scale of 0–4 as follows: 0, < 10%; 1, 10–25%; 2, 26–50%; 3, 50–75%; and 4, > 75%. The staining intensity was scored as 0–3 (Negative: 0; Weak expression: 1; Positive expression: 2; Strong expression: 3. The score represents the product of the positive staining

score, and the color intensity score was used as the final staining score for NAP1L1, Ki-67, and PCNA (0–12). For statistical analysis, final staining scores of 0–6 and 8–12 were considered to show low and high expression, respectively.

2.4 RT-PCR and QPCR

Total RNA was isolated from cells. CDNA was synthesized using reverse transcription reagents (TaKaRa Bio, Shiga, Japan), and cDNA was used as a template for amplification using specific primers (Table S1). Bio-Rad T100 and Bio-Rad CFX96 detection systems were applied for RT-PCR and QPCR, respectively, following the manufacturer's instructions.

2.5 Lentivirus infection

Lentiviral particles carrying the ShRNA-NAP1L1 precursor were provided by GeneChem (Shanghai, China). MCF-7 and MDA-MB-231 cells were infected with the lentiviral vector. The silencing efficiency for NAP1L1 was tested by Western blot analysis.

2.6 SiRNA and plasmid transfection

SiRNAs for NAP1L1 were designed and synthesized by RiboBio (Guangzhou, China). Plasmids for HDGF were obtained from Vigene Biosciences. Twelve hours before transfection, the breast cancer cells were plated into 6-well plates (Nest Biotech, China) and cultured to 30–50% confluence. SiRNAs or plasmids were then transfected at a concentration of 50 nM using the Lipofectamine 3000 Transfection Reagent (Invitrogen, Carlsbad, CA, USA) according to the manufacturer's protocol.

2.7 MTT assay

The breast cancer cells (2,000/well) were seeded into 96-well plates. For lentivirus-mediated shNAP1L1 expression, the cells were incubated for a week. For transient transfections with si-NAP1L1, the cells were cultured for four days. Subsequently, 20 μL of MTT (5 μg/μL in PBS) (Sigma, St Louis, MO) solution was added to each well and incubated for 4 h. Then, the formazan crystals formed by viable cells were solubilized in 150 mL dimethyl sulfoxide (Sigma, St Louis, MO), and the absorbance (OD) was measured at 490 nm. All the experiments were repeated at least three times.

2.8 Plate clone formation

Clone formation was studied following our previous study. The cells were seeded in 6-well culture plates at 500 cells/well. After incubation for 14 days, the cells were washed twice with D-Hanks solution and stained with hematoxylin solution. The number of colonies was counted under a microscope. All experiments were performed at least three times.

2.9 Edu staining

For the Edu incorporation assay, the proliferating breast cancer cells were examined using a Cell-Light Edu Apollo 488 or 567 In Vitro Imaging Kit (RiboBio) following the manufacturer's protocol. After incubation with 10 mM Edu for 2 h, the breast cancer cells were fixed with 4% paraformaldehyde,

permeabilized in 0.3% Triton X-100, and stained with Apollo fluorescent dyes. A total of 5 mg/mL of DAPI was used to stain the cell nuclei for 10 min. The number of Edu-positive cells was counted under a fluorescent microscope in five random fields. All assays were independently performed three times.

2.10 Subcutaneous tumorigenesis in nude mice

A total of 5×10^6 logarithmically growing breast cancer cells (MCF-7 and MDA-MB-231) carrying the ShRNA-NAP1L1 and their corresponding control cells were injected into the fourth pair of nude mice breast fat pads (BALB/C, nu/nu, female 3 weeks-old, one group = 5). The animals were fed an autoclaved laboratory rodent diet. On the 24th day, the tumor tissues were excised and weighed. All animal studies were conducted in accordance with the principles and procedures outlined in the Southern Medical University Guide for the Care and Use of Animals.

2.11 Western blot analysis

The extracted proteins were separated by 10% SDS-PAGE and further transferred onto PVDF membranes (Millipore, Bedford). Antibodies including NAP1L1 (1:1000; Proteintech, Rosemont, USA), CCND1 (1:1000; Proteintech, Rosemont, USA), HDGF (1:1000; Proteintech, Rosemont, USA), and c-Jun (1:1000; Proteintech, Rosemont, USA) were used in the Western blot assays based on the manufacturer's instructions. Detection was performed using the ECL Plus Western blotting detection reagents (Millipore, USA). The specific protein expression levels of the blots were normalized to GAPDH (1:1000; Bioworld, Nanjing, China).

2.12 Coimmunoprecipitation (Co-IP) assay

Co-IP was carried out using the Pierce Co-IP Kit (Thermos Scientific, USA) following the manufacturer's instructions. The total proteins were extracted and quantified. A total of 3000 specific protein expression levels of the blots were determined using normaanti-NAP1L1 (Abcam), anti-HDGF (Proteintech), anti-c-Jun (Proteintech), and anti-IgG antibodies for 12 h at 4 ℃. The beads were washed, eluted in a sample buffer, and boiled for 10 min at 100 ℃. The immune complexes were subjected to Coomassie Brilliant Blue staining and Western blot analysis. Anti-IgG was used as a negative control.

2.13 Confocal microscopy

The breast cancer cells were cultured overnight ($2ver^5$ /well) before they were fixed with 4% paraformaldehyde and permeabilized with 0.5% Triton X-100 at room temperature. The cells were incubated with anti-NAP1L1, anti-HDGF, and anti-c-Jun antibodies for 1 h at room temperature. After incubation for half an hour at 37 ℃ with a secondary antibody, coverslips were mounted onto the slides with a mounting solution containing 0.2 mg/mL DAPI. The images were captured by laser scanning confocal microscopy (Zeiss LSM 800).

2.14 Statistical analysis

Statistical analyses were carried out using the SPSS 20.0 statistical software package (SPSS, Chicago, IL, USA). Data are shown as the mean ± SD from at least three independent experiments. Two-tailed Student's t-test was applied for comparisons between groups. Survival analysis was performed using the Kaplan–Meier method. All statistical tests were two-sided; single, double, and triple asterisks indicate statistical significance (*P < 0.05, **P < 0.01, and ***P < 0.001).

3. Results

3.1 NAP1L1 overexpression promotes cell proliferation in breast cancer cells

According to the analysis of Clinical Proteomic Tumor Analysis Consortium (CPTAC) database, NAP1L1 protein was upregulated (Fig. 1A). Subsequently, we confirmed the upregulated protein levels by immunohistochemistry assay on clinic human breast cancer tissue sections (Fig. 1B). A tissue microarray (TMA) containing 97 breast cancer tissue samples and 10 breast tissues was used to perform NAP1L1 expression level, and cell staining scores were used to determine low and high expression (Fig. 1C, Table1).

Survival analysis showed that overexpressed NAP1L1 as an unfavorable factor that reduced the overall survival time of breast cancer patients (Fig. 1D). Then, the clinical significance of NAP1L1 expression was assessed (Table 2). Features associated with the survival in univariate Cox regression analysis were tumor scale (0.031), HER-2 (P = 0.014), NAP1L1 expression (P =0.001), and PR (P = 0.039). Furthermore, multivariate Cox regression analysis indicated that the high NAP1L1 expression level predicted poor survival compared with low NAP1L1 level (Table 3).

3.2 Downregulated NAP1L1 inhibits cell proliferation

Lentivirus-carrying shRNA-NAP1L1 was infected into MCF-7 and MDA-MB-231 cells. The *transfectionefficiency*was first analyzed by a real-time quantitative PCR (qRT-PCR) analysis (Fig. 2A), and *Western Blot* analysis was used to further validate the results (Fig. 2B). In addition, the MTT (Fig. 2C), plate clone (Fig. 2D), and EdU staining (Fig. 2E) assays confirmed that shNAP1L1 inhibits cell growth. Furthermore, an *invivo* study was carried out. The average weight and volume of tumors significantly decreased in the *xenograft mice after the injection of NAP1L1-decreasing breast cancer c*ells compared with the negative control group (Fig. 2F). Then, the ki-67 and PCNA expressions in xenograft tumors of nude mice were detected. The data show that the ki-67 and PCNA expression of the group injected with shRNA-NAP1L1 was significantly lower than that of the mock xenograft group (Fig. 2G).

3.3 SiRNA-NAP1L1 reduces cell proliferation *in vitro*

Knockdown *efficiency was* confirmed after transfecting siRNA-NAP1L1 to breast cancer cells (Figs. 3A and 3B). Then, MTT and EdU assays showed that the reduced NAP1L1 protein level significantly decreased the cell growth (Fig. 3C). EdU staining assay confirms the results obtained from *MTT* assay (Fig. 3D).

3.4 NAP1L1 interacts with HDGF

Endogenous Co-IP assay confirmed that NAP1L1 bound to HDGF(Figs. 4A and 4B). The confocal microscopic images showed the*colocalization*of NAP1L1 and HDGF*in* the*cytoplasm* of breast cancer cells (Fig. 4C).

3.5 HDGF recruits c-Jun

C-Jun was predicted as a potential interactor of HDGF based on the BioGrid database (https://thebiogrid.org/109928/summary/homo-sapiens/jun.html). In addition, the confocal microscopic images showed that HDGF interacts with c-Jun in the cytoplasm and nucleus (Fig. 5A). The Co-IP assay shows the interaction between c-Jun and HDGF in breast cancer (Figs. 5B and 5C).

3.6 Transfecting HDGF increases c-Jun/CCND1 signal and restores cell proliferation in NAP1L1-suppressing breast cancer cells

Furthermore, HDGF cDNA plasmid was transfected to NAP1L1-suppressing cells. The upregulated efficiency of HDGF was verified by qRT-PCR and Western blot analysis (Figs. 6A and 6B). According to our observation *in vitro*, the ability of cell proliferation (Fig. 6C) and EdU staining (Fig. 6D) was obviously restored. Western blot assay indicated that the intensity of c-Jun/CCND1 signal significantly increased (Fig. 6B).

3.7 C-Jun transfection enhances CCND1 signal and restores cell proliferation in NAP1L1-suppressing breast cancer cells

c-Jun cDNA plasmid was transfected to NAP1L1-suppressing cells. Using qRT-PCR and western blot (Fig. 7A,8B), significant mRNA and protein upregulation of c-Jun and CCND1 was observed. Furthermore, the ability of cell proliferation (Fig. 6C) and EdU staining (Fig. 6D) was restored *in vitro* in NAP1L1-suppressing breast cancer cells.

Discussion

In previous studies, NAP1L1 is reported to correlate with tumor pathogenesis. Zhai et al. found that miR-532-5p suppresses renal cancer cell proliferation by disrupting the ETS1-mediated positive feedback loop with the KRAS-NAP1L1/P-ERK axis. Chen et al. observed that PRDM8 suppresses the occurrence and development of hepatocellular carcinoma pathogenesis by targeting NAP1L1. Furthermore, elevated NAP1L1 expression was observed to promote carcinogenesis in colorectal cancer and pancreatic neuroendocrine neoplasm [10-14]. However, the role and molecular basis of NAP1L1 in breast cancer have never been documented.

To investigate the possible role of NAP1L1 in breast cancer, we first observed that the expression of NAP1L1 protein was significantly upregulated in breast cancer tissues compared to normal breast tissues based on the CPTAC database. Further, immunochemistry was used to detect the expression of NAP1L1 protein in breast cancer tissues and normal breast tissues. The data show a significant elevation of NAP1L1 protein expression in breast cancer tissues. Furthermore, an increase in NAP1L1 protein expression was found to be a predictor for poor survival prognosis in the high NAP1L1 expression group compared with the low expression group in breast cancer patients. Finally, multivariable analysis demonstrated that increased NAP1L1 expression is an independent prognosis marker for the overall survival in breast cancer. These data are consistent with the reported data on colorectal cancer[11,13], suggesting that NAP1L1 promotes the pathogenesis of breast cancer and might be a potential tumor promoter in breast cancer.

In previous studies, NAP1L1 was reported as a potential oncogene promoting cell growth[12,14]. Here, we also investigated the role of NAP1L1 in breast cancer cell growth. After suppressing NAP1L1 expression in breast cancer cells by using siRNA or lentivirus-mediated shRNA, it was observed that the ability of cell proliferation and EDU staining was significantly reduced. *In vivo* experiment showed that the ability of subcutaneous tumor formation of breast cancer cells significantly decreased after the expression of NAP1L1 was stably inhibited. The abovementioned data further supported NAP1L1 as a potential oncogene in breast cancer. This finding is consistent with the role of NAP1L1 in several tumors[10,12], indicating the importance of NAP1L1 in breast cancer pathogenesis. However, the molecular basis of NAP1L1 in breast cancer is still unclear.

In a previous study, we carried out Co-IP combined with mass spectrometry to search the potential interaction factors of HDGF in endometrial carcinoma (the data will be published in another paper). Interestingly, NAP1L1 was screened as one of the candidate interaction proteins of HDGF. HDGF was originally obtained from the conditioned media of HuH-7 hepatoma cells[15]. It has been widely reported as an oncogenic factor promoting tumor pathogenesis including NSCLC, endometrial cancer, nasopharyngeal carcinoma, breast cancer, and liver cancer in previous studies[16–21]. Anti-HDGF antibody treatment has been shown to enhance the antitumor activities of gemcitabine, bevacizumab, and chemotherapy in NSCLC [22,23]. These data indicate the significance of HDGF in tumor pathogenesis. Here, NAP1L1 was found to combine with HDGF by Co-IP examination in breast cancer cells. Furthermore,

it was confirmed that these two proteins are co-located in the cytoplasm of breast cancer. These data show that NAP1L1 interacts with HDGF in breast cancer

To further explore the molecular basis of NAP1L1 in inducing cell growth via HDGF, BioGrid database was used to predict the interactive proteins of HDGF. Excitingly, c-Jun was predicted as a potential candidate of HDGF. C-Jun is an oncogenic transcription factor stimulating the expression of some genes[24–28], which promotes the occurrence and development of many tumors. In this study, the interaction of HDGF with c-Jun was further confirmed using an endogenous Co-IP assay. Furthermore, HDGF and c-Jun were proved to be co-located in the cytoplasm and nucleus. This result indicated that HDGF recruits c-Jun to participate in tumor pathogenesis.

CCND1 is a significant cell cycle promoter inducing cell proliferation in tumors[29–31]. It is also a significant transcription product of c-Jun[32,33]. To prove whether CCND1 participated in NAP1L1/HGGF/c-Jun signal-induced cell proliferation, HDGF or c-Jun cDNA plasmid was transfected into shNAP1L1-treated breast cancer cells, and it was found that the c-Jun/CCND1 expression level was significantly upregulated in shNAP1L1-treated breast cancer cells. Furthermore, the cell proliferation ability was also restored in NAP1L1-suppressed breast cancer cells. These data demonstrated that HDGF/c-Jun/CCND1 signal positively participated in NAP1L1-induced breast cancer growth.

Taken together, an increased NAP1L1 protein level is an unfavorable outcome for breast cancer patients. It functions as a potential oncogene that interacts with HDGF to recruit c-Jun and thus stimulates CCND1 expression to induce cell cycle transition, finally promoting cell proliferation in breast cancer.

Declarations

Ethics approval and consent to participate

Not applicable.

Consent for publication

Not applicable.

Availability of data and materials

The datasets used during this study are available from the corresponding author on reasonable request.

Competing interests

The authors declare no conflict of interest.

Author contributions

GYY and BG planned the experiments and revised the paper. SEC, YWZ and SL performed the experiments and drafted the manuscript. QC and BL performed statistical analysis. YWZ conceived the project and edited the manuscript. BG and SEC discussed the results. All authors read and approved the final manuscript.

Acknowledgements

Not applicable.

Funding

This research did not receive any specific grant from funding agencies in the public, commercial, or not-for-profit sectors.

References

1. Zhou J, Wang H, Fu F, Li Z, Feng Q, Wu W, Liu Y, Wang C, Chen Y. Spectrum of PALB2 germline mutations and characteristics of PALB2-related breast cancer: Screening of 16,501 unselected patients with breast cancer and 5890 controls by next-generation sequencing. CANCER-AM CANCER SOC 2020, 126(14): 3202-3208.https://doi.org/10.1002/cncr.32905.
2. Gompel A. [Hormone and breast cancer]. PRESSE MED 2019, **48**(10)**:** 1085-1091.https://doi.org/10.1016/j.lpm.2019.09.021.
3. Engel C, Fischer C, Zachariae S, Bucksch K, Rhiem K, Giesecke J, Herold N, Wappenschmidt B, Hubbel V, Maringa M, Reichstein-Gnielinski S, Hahnen E, Bartram CR, Dikow N, Schott S, Speiser D, Horn D, Fallenberg EM, Kiechle M, Quante AS, Vesper AS, Fehm T, Mundhenke C, Arnold N, Leinert E, Just W, Siebers-Renelt U, Weigel S, Gehrig A, Wockel A, Schlegelberger B, Pertschy S, Kast K, Wimberger P, Briest S, Loeffler M, Bick U, Schmutzler RK. Breast cancer risk in BRCA1/2 mutation carriers and noncarriers under prospective intensified surveillance. INT J CANCER 2020, **146**(4)**:** 999-1009.https://doi.org/10.1002/ijc.32396.
4. Shoemaker ML, White MC, Wu M, Weir HK, Romieu I. Differences in breast cancer incidence among young women aged 20-49 years by stage and tumor characteristics, age, race, and ethnicity, 2004-2013. Breast Cancer Res Treat 2018, **169**(3)**:** 595-606.https://doi.org/10.1007/s10549-018-4699-9.
5. Brewer HR, Jones ME, Schoemaker MJ, Ashworth A, Swerdlow AJ. Family history and risk of breast cancer: an analysis accounting for family structure. Breast Cancer Res Treat 2017, **165**(1)**:** 193-200.https://doi.org/10.1007/s10549-017-4325-2.
6. Jacquez GM, Barlow J, Rommel R, Kaufmann A, Rienti MJ, AvRuskin G, Rasul J. Residential mobility and breast cancer in Marin County, California, USA. Int J Environ Res Public Health 2013, **11**(1)**:** 271-295.https://doi.org/10.3390/ijerph110100271.
7. Attia M, Forster A, Rachez C, Freemont P, Avner P, Rogner UC. Interaction between nucleosome assembly protein 1-like family members. J MOL BIOL 2011, 407(5): 647-

660.https://doi.org/10.1016/j.jmb.2011.02.016.

8. Gupta N, Thakker S, Verma SC. KSHV encoded LANA recruits Nucleosome Assembly Protein NAP1L1 for regulating viral DNA replication and transcription. Sci Rep 2016, **6:** 32633.https://doi.org/10.1038/srep32633.
9. Qiao H, Li Y, Feng C, Duo S, Ji F, Jiao J. Nap1l1 Controls Embryonic Neural Progenitor Cell Proliferation and Differentiation in the Developing Brain. CELL REP 2018, **22**(9)**:** 2279-2293.https://doi.org/10.1016/j.celrep.2018.02.019.
10. Zhai W, Ma J, Zhu R, Xu C, Zhang J, Chen Y, Chen Z, Gong D, Zheng J, Chen C, Li S, Li B, Huang Y, Xue W, Zheng J. MiR-532-5p suppresses renal cancer cell proliferation by disrupting the ETS1-mediated positive feedback loop with the KRAS-NAP1L1/P-ERK axis. Br J Cancer 2018, **119**(5)**:** 591-604.https://doi.org/10.1038/s41416-018-0196-5.
11. Queiroz C, Song F, Reed KR, Al-Khafaji N, Clarke AR, Vimalachandran D, Miyajima F, Pritchard DM, Jenkins JR. NAP1L1: A Novel Human Colorectal Cancer Biomarker Derived From Animal Models of Apc Inactivation. FRONT ONCOL 2020, **10:** 1565.https://doi.org/10.3389/fonc.2020.01565.
12. Chen Z, Gao W, Pu L, Zhang L, Han G, Zuo X, Zhang Y, Li X, Shen H, Wu J, Wang X. PRDM8 exhibits antitumor activities toward hepatocellular carcinoma by targeting NAP1L1. HEPATOLOGY 2018, **68**(3)**:** 994-1009.https://doi.org/10.1002/hep.29890.
13. Nagashio R, Kuchitsu Y, Igawa S, Kusuhara S, Naoki K, Satoh Y, Ichinoe M, Murakumo Y, Saegusa M, Sato Y. Prognostic significance of NAP1L1 expression in patients with early lung adenocarcinoma. Biomed Res 2020, **41**(3)**:** 149-159.https://doi.org/10.2220/biomedres.41.149.
14. Schimmack S, Taylor A, Lawrence B, Alaimo D, Schmitz-Winnenthal H, Buchler MW, Modlin IM, Kidd M. A mechanistic role for the chromatin modulator, NAP1L1, in pancreatic neuroendocrine neoplasm proliferation and metastases. Epigenetics Chromatin 2014, **7:** 15.https://doi.org/10.1186/1756-8935-7-15.
15. Nakamura H, Kambe H, Egawa T, Kimura Y, Ito H, Hayashi E, Yamamoto H, Sato J, Kishimoto S. Partial purification and characterization of human hepatoma-derived growth factor. CLIN CHIM ACTA 1989, **183**(3)**:** 273-284.https://doi.org/10.1016/0009-8981(89)90361-6.
16. Liu C, Wang L, Jiang Q, Zhang J, Zhu L, Lin L, Jiang H, Lin D, Xiao Y, Fang W, Guo S. Hepatoma-Derived Growth Factor and DDX5 Promote Carcinogenesis and Progression of Endometrial Cancer by Activating beta-Catenin. FRONT ONCOL 2019, **9:** 211.https://doi.org/10.3389/fonc.2019.00211.
17. Chen SC, Kung ML, Hu TH, Chen HY, Wu JC, Kuo HM, Tsai HE, Lin YW, Wen ZH, Liu JK, Yeh MH, Tai MH. Hepatoma-derived growth factor regulates breast cancer cell invasion by modulating epithelial–mesenchymal transition. J PATHOL 2012, **228**(2)**:** 158-169.https://doi.org/10.1002/path.3988.
18. Wang S, Fang W. Increased expression of hepatoma-derived growth factor correlates with poor prognosis in human nasopharyngeal carcinoma. HISTOPATHOLOGY 2011, **58**(2)**:** 217-224.https://doi.org/10.1111/j.1365-2559.2010.03739.x.
19. Fu Q, Song X, Liu Z, Deng X, Luo R, Ge C, Li R, Li Z, Zhao M, Chen Y, Lin X, Zhang Q, Fang W. miRomics and Proteomics Reveal a miR-296-3p/PRKCA/FAK/Ras/c-Myc Feedback Loop Modulated

by HDGF/DDX5/beta-catenin Complex in Lung Adenocarcinoma. CLIN CANCER RES 2017, **23**(20)**:** 6336-6350.https://doi.org/10.1158/1078-0432.CCR-16-2813.

20. Min X, Wen J, Zhao L, Wang K, Li Q, Huang G, Liu J, Zhao X. Role of hepatoma-derived growth factor in promoting de novo lipogenesis and tumorigenesis in hepatocellular carcinoma. MOL ONCOL 2018, **12**(9)**:** 1480-1497.https://doi.org/10.1002/1878-0261.12357.
21. Xiao YY, Lin L, Li YH, Jiang HP, Zhu LT, Deng YR, Lin D, Chen W, Zeng CY, Wang LJ, Chen SC, Jiang QP, Liu CH, Fang WY, Guo SQ. ZEB1 promotes invasion and metastasis of endometrial cancer by interacting with HDGF and inducing its transcription. AM J CANCER RES 2019, **9**(11)**:** 2314-2330.
22. Ren H, Chu Z, Mao L. Antibodies targeting hepatoma-derived growth factor as a novel strategy in treating lung cancer. MOL CANCER THER 2009, **8**(5)**:** 1106-1112.https://doi.org/10.1158/1535-7163.MCT-08-0779.
23. Zhao J, Ma MZ, Ren H, Liu Z, Edelman MJ, Pan H, Mao L. Anti-HDGF targets cancer and cancer stromal stem cells resistant to chemotherapy. CLIN CANCER RES 2013, **19**(13)**:** 3567-3576.https://doi.org/10.1158/1078-0432.CCR-12-3478.
24. Liu Y, Jiang Q, Liu X, Lin X, Tang Z, Liu C, Zhou J, Zhao M, Li X, Cheng Z, Li L, Xie Y, Liu Z, Fang W. Cinobufotalin powerfully reversed EBV-miR-BART22-induced cisplatin resistance via stimulating MAP2K4 to antagonize non-muscle myosin heavy chain IIA/glycogen synthase 3beta/beta-catenin signaling pathway. EBIOMEDICINE 2019, **48:** 386-404.https://doi.org/10.1016/j.ebiom.2019.08.040.
25. Lin X, Zuo S, Luo R, Li Y, Yu G, Zou Y, Zhou Y, Liu Z, Liu Y, Hu Y, Xie Y, Fang W, Liu Z. HBX-induced miR-5188 impairs FOXO1 to stimulate beta-catenin nuclear translocation and promotes tumor stemness in hepatocellular carcinoma. THERANOSTICS 2019, **9**(25)**:** 7583-7598.https://doi.org/10.7150/thno.37717.
26. Liu C, Peng X, Li Y, Liu S, Hou R, Zhang Y, Zuo S, Liu Z, Luo R, Li L, Fang W. Positive feedback loop of FAM83A/PI3K/AKT/c-Jun induces migration, invasion and metastasis in hepatocellular carcinoma. BIOMED PHARMACOTHER 2020, **123:** 109780.https://doi.org/10.1016/j.biopha.2019.109780.
27. Lin X, Li AM, Li YH, Luo RC, Zou YJ, Liu YY, Liu C, Xie YY, Zuo S, Liu Z, Liu Z, Fang WY. Silencing MYH9 blocks HBx-induced GSK3beta ubiquitination and degradation to inhibit tumor stemness in hepatocellular carcinoma. Signal Transduct Target Ther 2020, **5**(1)**:** 13.https://doi.org/10.1038/s41392-020-0111-4.
28. Zou Y, Lin X, Bu J, Lin Z, Chen Y, Qiu Y, Mo H, Tang Y, Fang W, Wu Z. Timeless-Stimulated miR-5188-FOXO1/beta-Catenin-c-Jun Feedback Loop Promotes Stemness via Ubiquitination of beta-Catenin in Breast Cancer. MOL THER 2020, **28**(1)**:** 313-327.https://doi.org/10.1016/j.ymthe.2019.08.015.
29. Zhao M, Xu P, Liu Z, Zhen Y, Chen Y, Liu Y, Fu Q, Deng X, Liang Z, Li Y, Lin X, Fang W. Dual roles of miR-374a by modulated c-Jun respectively targets CCND1-inducing PI3K/AKT signal and PTEN-suppressing Wnt/beta-catenin signaling in non-small-cell lung cancer. CELL DEATH DIS 2018, **9**(2)**:** 78.https://doi.org/10.1038/s41419-017-0103-7.
30. Ai B, Kong X, Wang X, Zhang K, Yang X, Zhai J, Gao R, Qi Y, Wang J, Wang Z, Fang Y. LINC01355 suppresses breast cancer growth through FOXO3-mediated transcriptional repression of CCND1.

CELL DEATH DIS 2019, **10**(7)**:** 502.https://doi.org/10.1038/s41419-019-1741-8.

31. Zhen Y, Fang W, Zhao M, Luo R, Liu Y, Fu Q, Chen Y, Cheng C, Zhang Y, Liu Z. miR-374a-CCND1-pPI3K/AKT-c-JUN feedback loop modulated by PDCD4 suppresses cell growth, metastasis, and sensitizes nasopharyngeal carcinoma to cisplatin. ONCOGENE 2017, **36**(2)**:** 275-285.https://doi.org/10.1038/onc.2016.201.
32. Ouafik L, Berenguer-Daize C, Berthois Y. Adrenomedullin promotes cell cycle transit and up-regulates cyclin D1 protein level in human glioblastoma cells through the activation of c-Jun/JNK/AP-1 signal transduction pathway. CELL SIGNAL 2009, **21**(4)**:** 597-608.https://doi.org/10.1016/j.cellsig.2009.01.001.
33. Cicatiello L, Addeo R, Sasso A, Altucci L, Petrizzi VB, Borgo R, Cancemi M, Caporali S, Caristi S, Scafoglio C, Teti D, Bresciani F, Perillo B, Weisz A. Estrogens and progesterone promote persistent CCND1 gene activation during G1 by inducing transcriptional derepression via c-Jun/c-Fos/estrogen receptor (progesterone receptor) complex assembly to a distal regulatory element and recruitment of cyclin D1 to its own gene promoter. MOL CELL BIOL 2004, **24**(16)**:** 7260-7274.https://doi.org/10.1128/MCB.24.16.7260-7274.2004.

Tables

Table 1.The expression of NAP1L1 in breast cancer and adjacent tissues

Group	Case(n)	NAP1L1 expression		P-value*
		Low	High	
Breast cancer	97	72（74.2%）	25（25.8%）	p<0.001
Adjacent	10	9（90%）	1（10%）	

χ^2-test was applied to access the expression of NAP1L1.

Table.2 Correlation of NAP1L1 expression with clinicopathological characteristics of patients with Breast cancer

Characteristics	n	NAP1L1 expression		
		High	Low	p
Age(year)				
<50	43	15(34.9%)	28(65.1%)	0.067
≥50	54	10(%)	44(%)	
Clinical stage				
	8	1(12.5%)	7(87.5%)	0.370
~	89	24(27.0%)	65(73.0%)	
Tumor scale				
≤3cm	53	13(24.5%)	40(75.5%)	0.758
>3cm	44	12(27.3%)	32(72.7%)	
Histological Grade				
	29	9(31.0%)	20(69.0%)	0.439
~	68	16(23.5%)	52(76.5%)	
Vital states				
Die	26	13(50.0%)	13(50.0%)	0.001
Alive	71	12(16.9%)	59(83.1%)	
ER				
Negative	36	12(33.3%)	24(66.7%)	0.191
Positive	61	13(21.3%)	48(78.7%)	
PR				
Negative	40	14(35.0%)	26(65.0%)	0.082
Positive	57	11(19.3%)	46(80.7%)	
HER2				
Negative	60	15(25.0%)	45(75.0%)	0.825
Positive	37	10(27.0%)	27(73.0%)	
Lymph metastasis metastasismetastasis				

No	32	6(18.8%)	26(81.2%)	0.267
Yes	65	19(29.2%)	46(70.8%)	

Table.3 Summary of univariate and multivariate Cox regression analysis

Parameter	Univariate analysis			Multivariate analysis		
	Hazard Ratio	95.0% CI	p	Hazard Ratio	95.0% CI	p
Age(year)	1.216	0.551-2.687	0.628			
Clinical stage	23.370	0.064-8597.978	0.296			
Tumor scale	1.000	0.454-2.202	0.999			
Histological Grade	0.832	0.395-1.929	0.668			
ER	0.548	0.254-1.185	0.126			
PR	0.439	0.201-0.958	0.039	0.554	0.249-1.232	0.147
HER2	1.553	0.717-3.361	0.264			
Lymph metastasis	0.989	0.441-2.221	0.979			
NAP1L1 expression	3.851	1.754-8.455	0.001	3.381	1.512-7.559	0.003

Figures

g 1

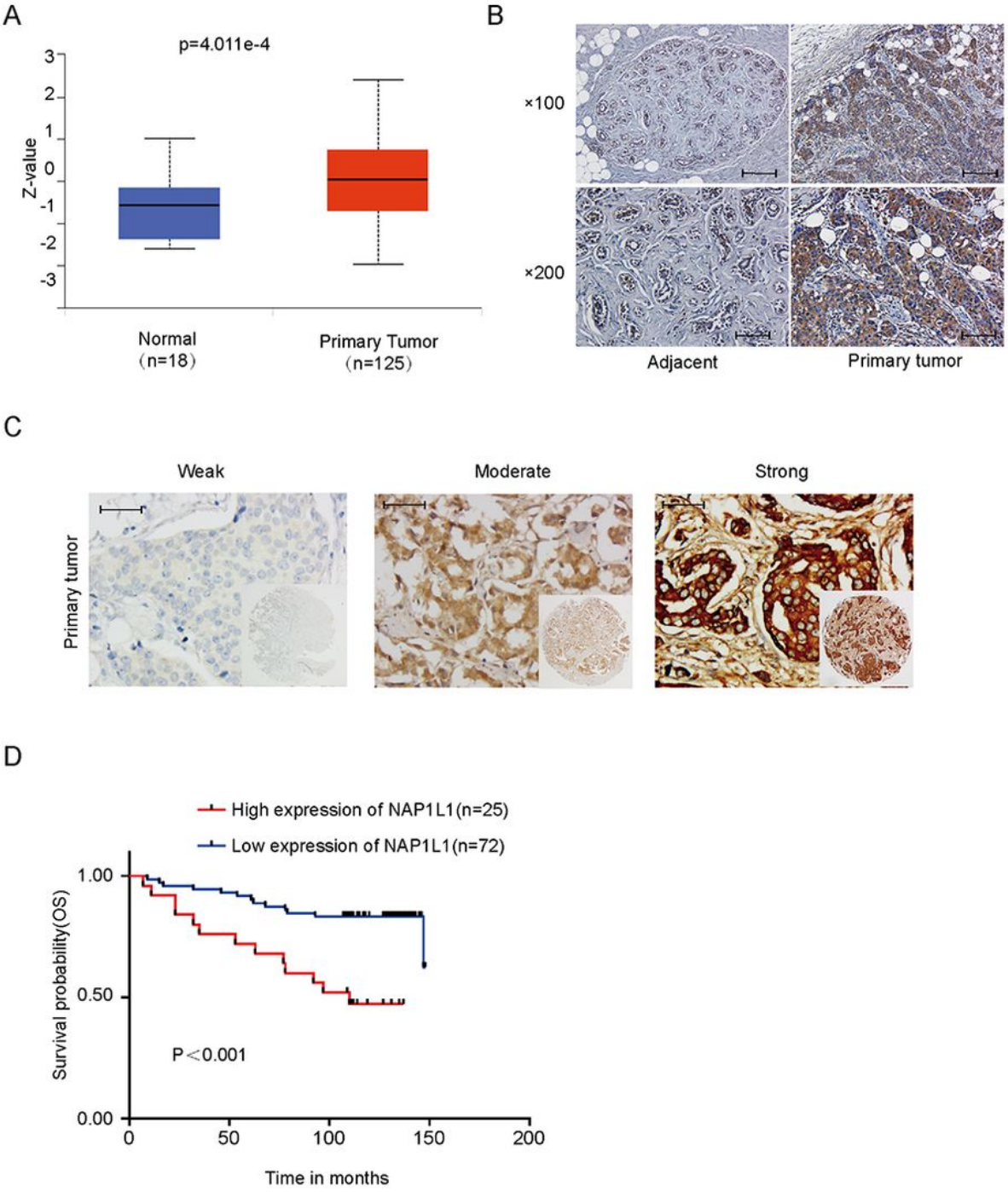

Figure 1

Expression of NAP1L1 in breast cancer A: NAP1L1 protein expression in breast cancer in CPTAC (http://ualcan.path.uab.edu/) (Z-values represent standard deviations from the median across samples for the given cancer type. The Log2 spectral count ratios obtained from CPTAC were first normalized within each sample profile and then normalized across samples). B: NAP1L1 expression was measured via immunohistochemical staining in breast cancer and paracarcinoma tissues (100× visual field scale

bar: 200 μm 200× visual field scale bar: 100 μm). C: NAP1L1 expression performed in TMA (scale bar: 50 μm).D: Kaplan–Meier survival analysis for the overall survival in TMA performed NAP1L1 expression. Data are presented as mean±s.d. from three independent experiments. *P < 0.05 vs. control; **P < 0.01; ***P < 0.001.

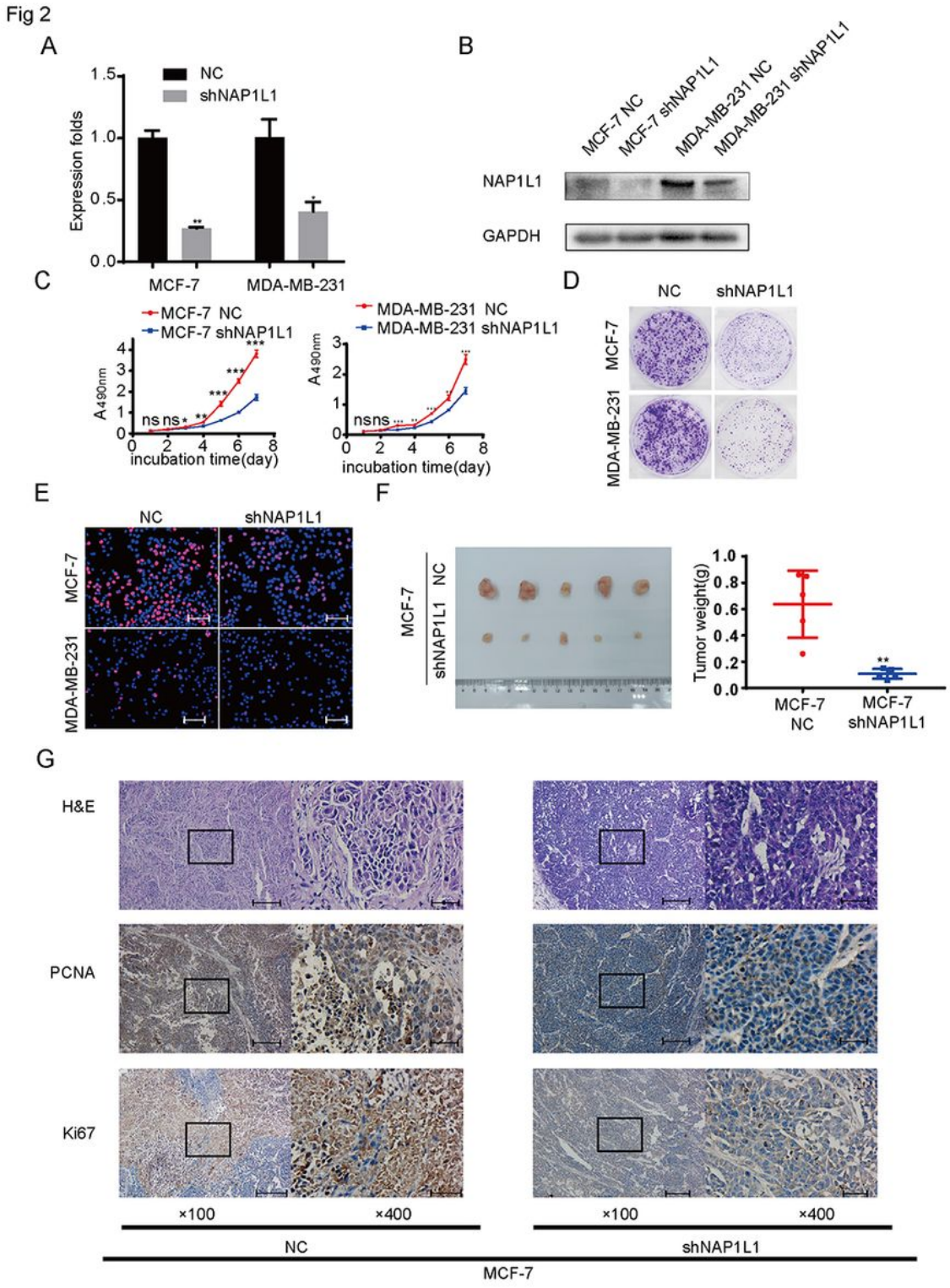

Figure 2

Stably downregulated NAP1L1 attenuated breast cancer cell proliferation A: RT-qPCR to measure the NAP1L1 mRNA expression after shRNA-NAP1L1 lentivirus or negative control (NC) lentivirus transfection into breast cancer cells. B: Efficiency for silencing NAP1L1 protein was measured by Western blot analysis. C: MTT assay indicated that shRNA-NAP1L1 inhibited the cell proliferation in breast cancer cells. D: Knockdown of NAP1L1 expression suppressed the plate clone formation in vitro. E: Downregulation of NAP1L1 suppresses EdU staining of breast cancer (scale bar: 200 μm). F: Xenograft tumor of nude mice showed that the average weight and volume of tumors decreased in shRNA-NAP1L1 group compared with the negative control group. G: Expression levels of PCNA and Ki-67 were measured via IHC staining in the xenograft tumor of nude mice(100× visual field scale bar: 200 μm, 400e bar: bar: 50 μm). The data are presented as mean±s.d. from three independent experiments. *P < 0.05 vs. control; **P < 0.01; ***P < 0.001.

Fig 3

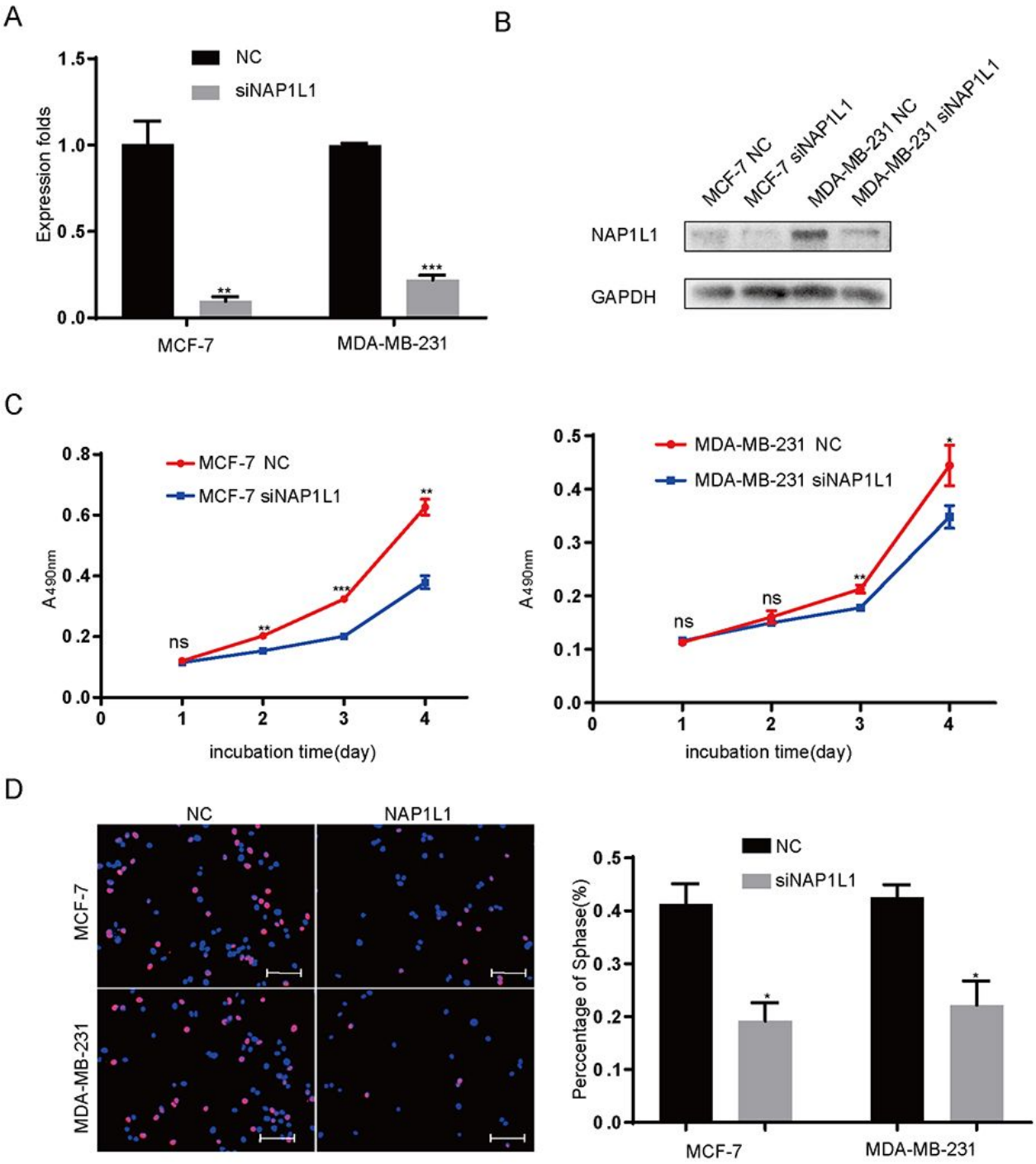

Figure 3

SiRNA-NAP1L1 reduces cell proliferation in vitro A: RT-qPCR for measuring NAP1L1 mRNA expression after siRNA-NAP1L1 or NC siRNA-control transfection into breast cancer cells. B: Expression levels of NAP1L1 protein were detected by Western blot analysis to screen the effectiveness of siRNA-NAP1L1 fragments. C: MTT assays showed that the inhibition of NAP1L1 reduces cell proliferation in vitro in breast cancer MCF-7 and MDA-MB-231 cell lines. D: Downregulation of NAP1L1 suppressed the EdU

staining of breast cancer cells in vitro (scale bar: 200 μm). The data are presented as mean±s.d. from three independent experiments. *P < 0.05 vs. control; **P < 0.01; ***P < 0.001.

Fig 4

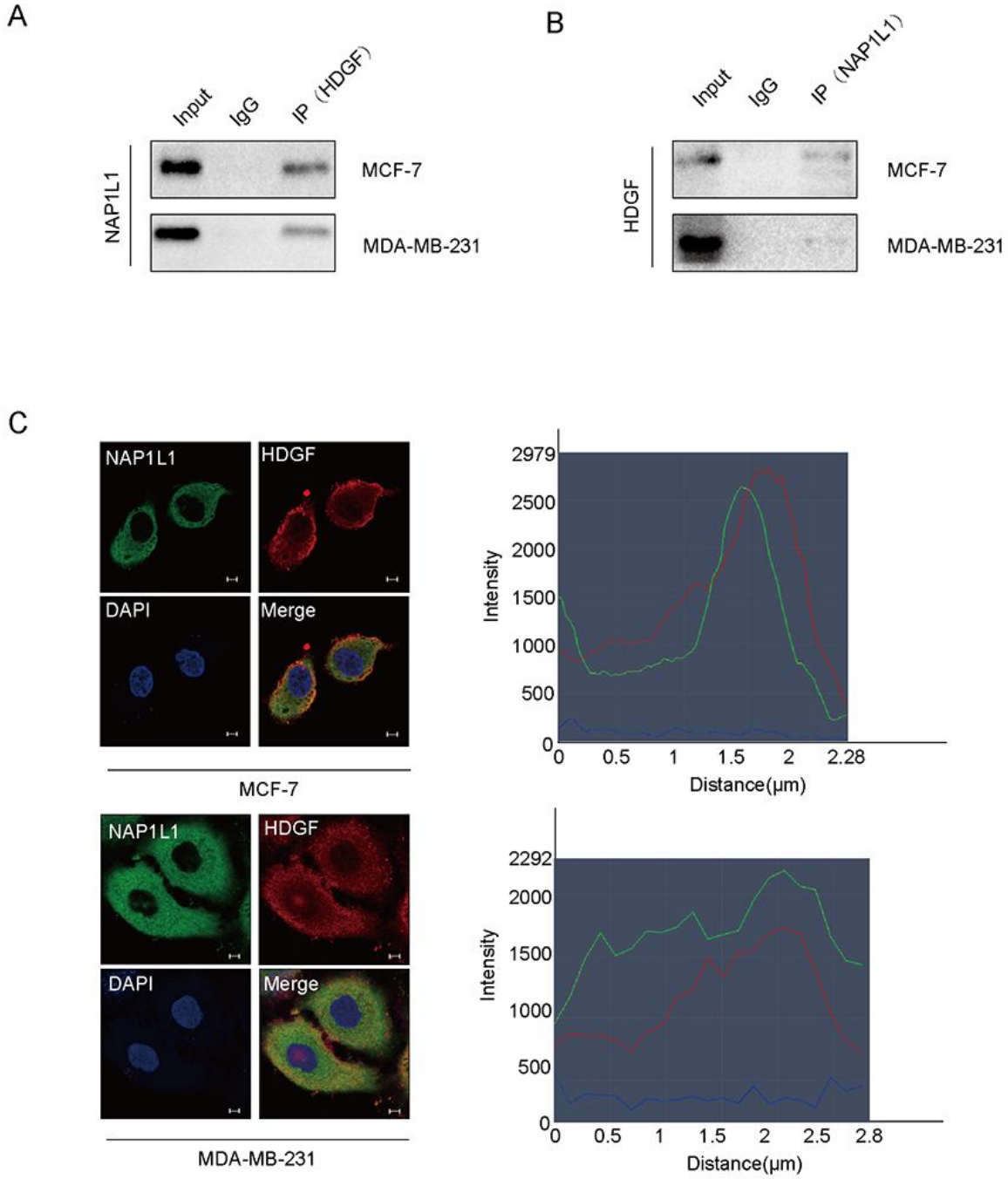

Figure 4

NAP1L1 interacts with HDGF A: Co-IP assay was performed to identify the interaction of NAP1L1 with HDGF. B: Confocal microscopic images showed the colocalization of NAP1L1 with HDGF in the cytoplasm of breast cancer cells (scale bar: 5 μm).

Fig 5

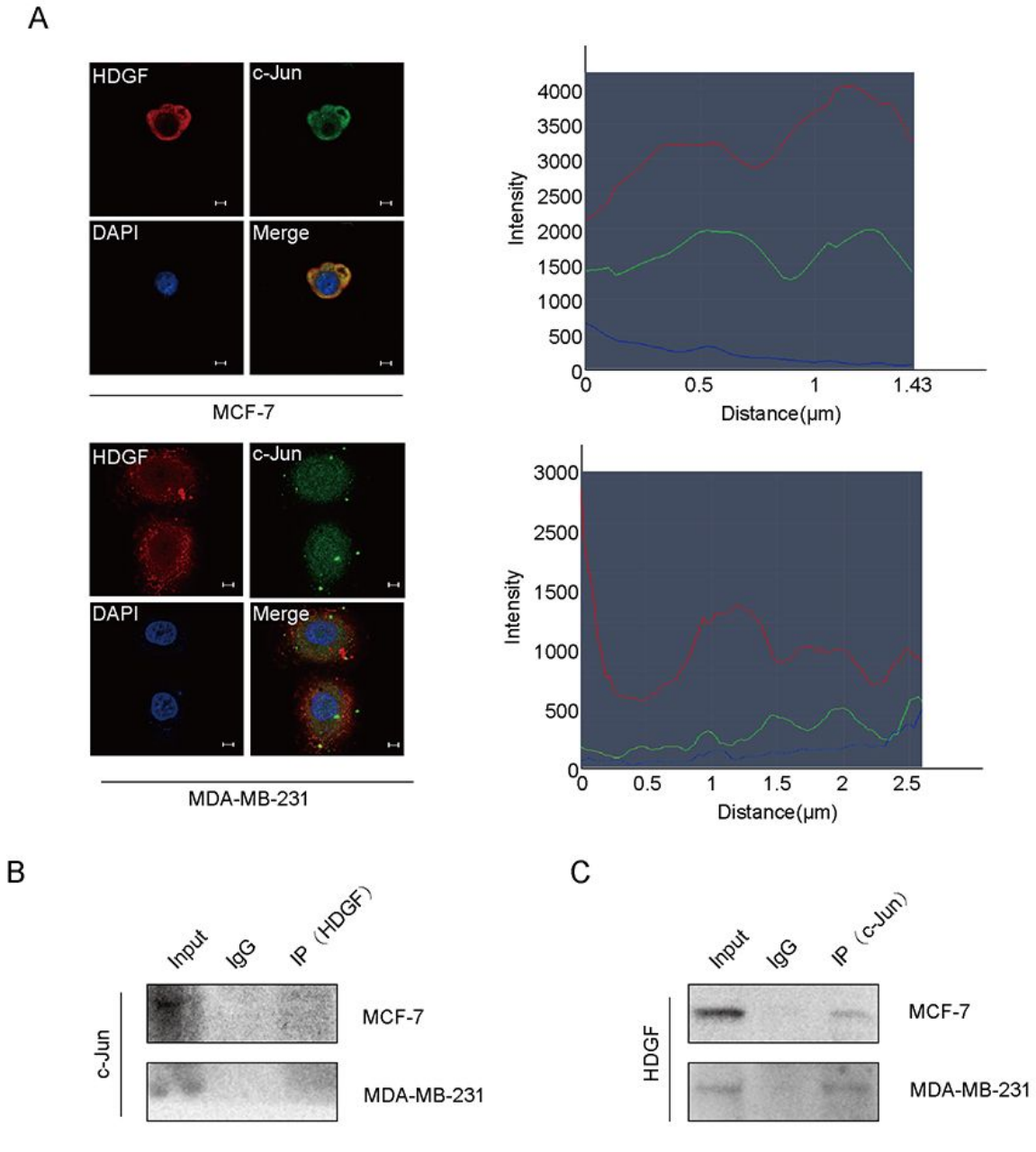

Figure 5

HDGF recruits c-Jun. A: Co-IP assay was performed to identify the interaction of HDGF with c-Jun. B: Confocal microscopic images showed the colocalization of HDGF and c-Jun in the cytoplasm and nucleus in breast cancer cells (scale bar: 5 μm).

Fig 6

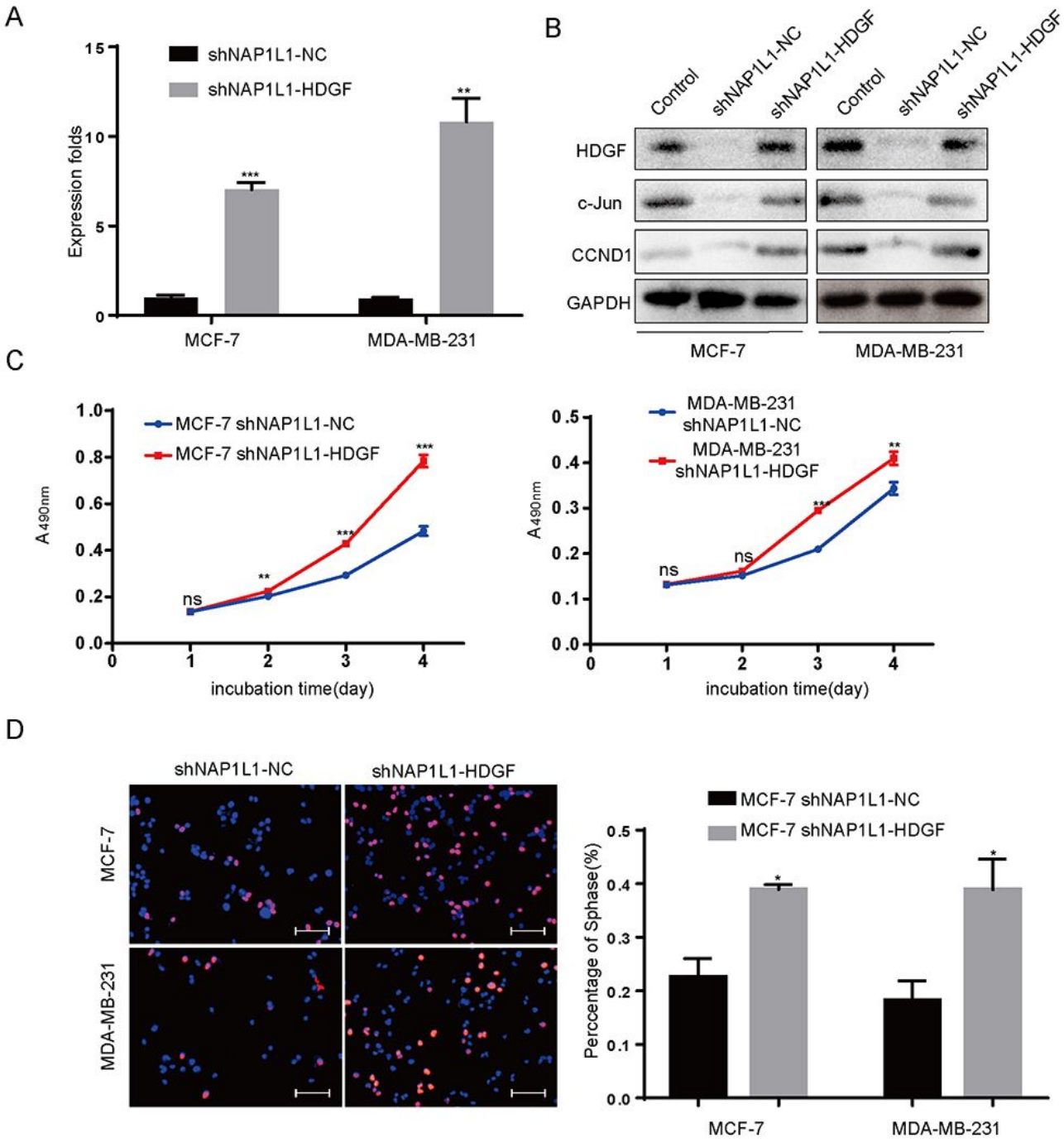

Figure 6

Transfecting HDGF restores the cell proliferation in NAP1L1-suppressing breast cancer cells through c-Jun/CCND1 signal. A: NAP1L1, HDGF, c-Jun, and CCND1 protein levels were evaluated in NC, shNAP1L1, and HDGF-shNAP1L1 breast cancer cells. B: RT-qPCR data was used to measure the HDGF expression after restoring HDGF in shNAP1L1 breast cancer cells. C: MTT assays indicated that transfecting HDGF restores the cell growth of breast cancer. D: Transfecting HDGF restores EdU staining of breast cancer

(scale bar: 200 μm). The data are presented as mean±s.d. from three independent experiments. *P < 0.05 vs. control; **P < 0.01; ***P < 0.001.

Fig 7

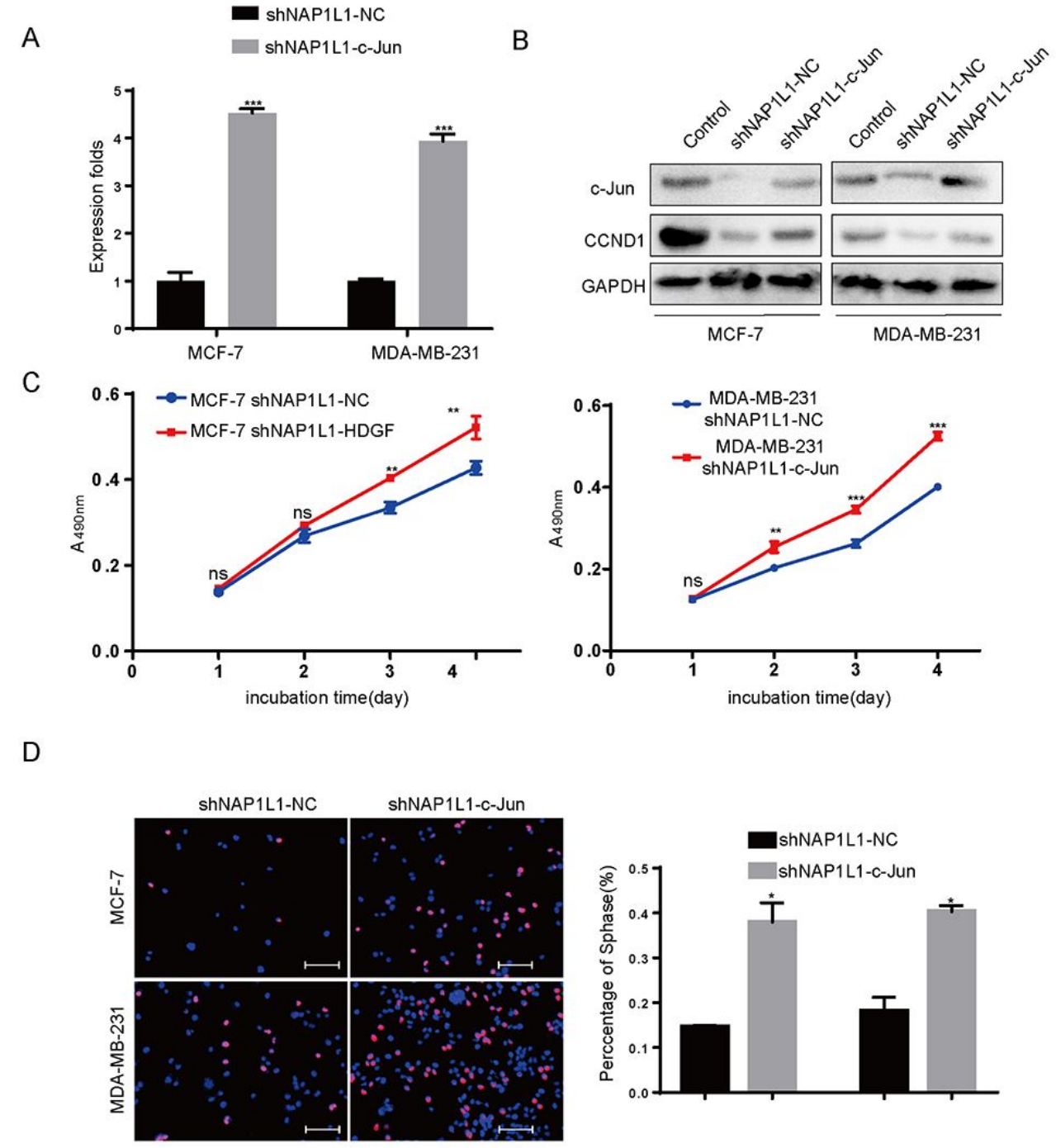

Figure 7

Transfecting c-Jun increases the CCND1 signal and restores the cell growth in NAP1L1-suppressing breast cancer cells. A: RT-qPCR was used to measure the c-Jun expression after restoring c-Jun in NC, shNAP1L1, and c-Jun-shNAP1L1 of breast cancer cells. B: C-Jun and CCND1 protein levels were

measured when c-Jun was transfected in shNAP1L1-breast cancer cells (scale bar: 200 μm). C: MTT assays showed that transfecting c-Jun restores the cell proliferation of breast cancer cells. D: EdU assay showed that transfecting c-Jun restores the cell cycle progression (scale bar: 200 μm). *P < 0.05 vs. control; **P < 0.01; ***P < 0.001.

Supplementary Files

This is a list of supplementary files associated with this preprint. Click to download.

- TableS1.doc
- TableS2.doc
- TableS3.doc